RLIM Is a Candidate Dosage-Sensitive Gene for Individuals with Varying Duplications of Xq13, Intellectual Disability, and Distinct Facial Features

Elizabeth E. Palmer,[1,2,3,4,24,*] Renee Carroll,[5,24] Marie Shaw,[5] Raman Kumar,[5] Andre E. Minoche,[6] Melanie Leffler,[1] Lucinda Murray,[1] Rebecca Macintosh,[3] Dale Wright,[7,8] Chris Troedson,[9] Fiona McKenzie,[10,11] Sharron Townshend,[11] Michelle Ward,[11] Urwah Nawaz,[5] Anja Ravine,[8,12] Cassandra K. Runke,[13] Erik C. Thorland,[13] Marybeth Hummel,[14] Nicola Foulds,[15] Olivier Pichon,[16] Bertrand Isidor,[16] Cédric Le Caignec,[17] Bénédicte Demeer,[18,19] Joris Andrieux,[20] Salam Hadah Albarazi,[21] Ann Bye,[2,3] Rani Sachdev,[2,3] Edwin P. Kirk,[2,3] Mark J. Cowley,[22] Mike Field,[1] and Jozef Gecz[5,23,*]

Summary

Interpretation of the significance of maternally inherited X chromosome variants in males with neurocognitive phenotypes continues to present a challenge to clinical geneticists and diagnostic laboratories. Here we report 14 males from 9 families with duplications at the Xq13.2-q13.3 locus with a common facial phenotype, intellectual disability (ID), distinctive behavioral features, and a seizure disorder in two cases. All tested carrier mothers had normal intelligence. The duplication arose *de novo* in three mothers where grandparental testing was possible. In one family the duplication segregated with ID across three generations. *RLIM* is the only gene common to our duplications. However, flanking genes duplicated in some but not all the affected individuals included the brain-expressed genes *NEXMIF*, *SLC16A2*, and the long non-coding RNA gene *FTX*. The contribution of the *RLIM*-flanking genes to the phenotypes of individuals with different size duplications has not been fully resolved. Missense variants in *RLIM* have recently been identified to cause X-linked ID in males, with heterozygous females typically having normal intelligence and highly skewed X chromosome inactivation. We detected consistent and significant increase of *RLIM* mRNA and protein levels in cells derived from seven affected males from five families with the duplication. Subsequent analysis of MDM2, one of the targets of the RLIM E3 ligase activity, showed consistent downregulation in cells from the affected males. All the carrier mothers displayed normal *RLIM* mRNA levels and had highly skewed X chromosome inactivation. We propose that duplications at Xq13.2-13.3 including *RLIM* cause a recognizable but mild neurocognitive phenotype in hemizygous males.

Structural or sequence variants affecting X chromosome genes account for 5%–10% of all intellectual disability (ID) in males and a higher proportion of ID in multigenerational families with affected males.[1] The assessment of pathogenicity of previously unreported X chromosomal variants can be challenging, particularly because heterozygous female carriers are often unaffected. However, correct interpretation of the pathogenicity of X chromosome variants is critical not only to allow accurate genetic counseling for the carrier mother but also for the extended family that may include several unaffected female carriers.[2]

RLIM (MIM: 300379) was recently identified as a putative X linked ID (XLID) gene in a three-generation Norwegian family (Tonne-Kalscheuer syndrome, TOKAS [MIM: 300978]).[3] A rare missense variant (GenBank: NM_016120.4 [*RLIM*]; c.1067A>G [p.Tyr356Cys]) segregated with a phenotype in males with subtle facial dysmorphism, autism, and feeding problems. Hu et al.[4] reported missense variants segregating with ID in three large XLID-affected families. Recently, Frints et al.[5] further delineated the neurodevelopmental phenotype in nine families with *RLIM* missense variants, confirming a role of *RLIM* in neurodevelopmental conditions with the core clinical presentation of ID. Frints

[1]Genetics of Learning Disability Service, Waratah, NSW 2298, Australia; [2]School of Women's and Children's Health, UNSW Medicine, University of New South Wales, Randwick, NSW 2031, Australia; [3]Sydney Children's Hospital, Randwick, NSW 2031, Australia; [4]Kinghorn Centre for Clinical Genomics, Garvan Institute, Darlinghurst, Sydney, NSW 2010, Australia; [5]Adelaide Medical School and the Robinson Research Institute, University of Adelaide, Adelaide, SA 5000, Australia; [6]St Vincent's Clinical School, University of New South Wales, Sydney, NSW 2010, Australia; [7]Discipline of Genomic Medicine and Discipline of Child & Adolescent Health, University of Sydney, Sydney, NSW 2010, Australia; [8]Department of Cytogenetics, The Children's Hospital at Westmead, Westmead, NSW 2145, Australia; [9]Children's Hospital at Westmead, Sydney, NSW 2145, Australia; [10]School of Paediatrics and Child Health, University of Western Australia, Perth, WA 6009, Australia; [11]Genetic Services of Western Australia, Perth, WA 6008, Australia; [12]Pathwest Laboratory Medicine WA, Perth, WA 6008, Australia; [13]Genomics Laboratory, Department of Laboratory Medicine and Pathology, Mayo Clinic, Scottsdale, AZ 85259, USA; [14]West Virginia University School of Medicine, Department of Pediatrics, Section of Medical Genetics Morgantown, WV 26506-9600, USA; [15]Wessex Clinical Genetics Services, Southampton SO16 5YA, UK; [16]Service de génétique médicale - Unité de Génétique Clinique, CHU de Nantes - Hôtel Dieu, Nantes 44093, France; [17]Service de génétique médicale, Institut fédératif de Biologie, CHU Hopital Purpan, Toulouse 31059, France; [18]Center for Human Genetics, CLAD Nord de France, CHU Amiens-Picardie, Amiens 80080, France; [19]CHIMERE EA 7516, University Picardie Jules Verne, Amiens 80025, France; [20]Institut de Biochimie et Génétique Moléculaire, CHU Lille, Lille 59000, France; [21]Hospital Center De Saint-Quentin, Saint-Quentin 02321, France; [22]Children's Cancer Institute, Lowy Cancer Research Centre, University of New South Wales, Randwick, NSW 2033, Australia; [23]Healthy Mothers, Babies and Children, South Australian Health and Medical Research Institute, Adelaide, SA 5000, Australia
[24]These authors contributed equally to this work
*Correspondence: elizabeth.palmer@health.nsw.gov.au (E.E.P.), jozef.gecz@adelaide.edu.au (J.G.)
https://doi.org/10.1016/j.ajhg.2020.10.005.

and colleagues described typical clinical features in the affected males with mild growth retardation of prenatal onset, ID of variable severity, hypogenitalism, and subtle facial features including (relative) microcephaly and hypertelorism in childhood evolving to hypotelorism in adulthood. Although they reported autistic features and hyperactivity, children were also frequently described as friendly. With age, more difficult behaviors, including aggressive outbursts and anxiety, depression, and schizophrenia, were reported.[5] To date all reported carrier females had normal cognition and behavior but a few had minor distinctive physical features, including short stature. All tested carrier females had skewed X chromosome inactivation with the X chromosome carrying the missense variant being selectively inactivated.

RLIM encodes a RING (really interesting new gene) domain-containing zinc-finger E3 ubiquitin ligase shown to act as a co-factor promoting or inhibiting transcription via binding to LIM-homeodomain (LIM-HD) transcription factors. RLIM acts as a recruiter of the Sin3A/histone deacetylase corepressor complex and an E3 ubiquitin ligase, ubiquitinating target proteins for degradation by the proteasome.[5,6] Pathogenic variants in multiple E3 ubiquitin ligase coding genes, such as *HERC2* (MIM: 605837),[7] *CUL4B* (MIM: 300304),[8] *HUWE1* (MIM: 300697),[9] *TRIP12* (MIM: 604506),[10] and *UBE3A* (MIM: 601623),[11] have been identified in individuals with ID. RLIM has diverse but incompletely understood functions. RLIM is involved in control of early embryogenesis, notably brain and neural tube development. It also has a role in control of cell migration, for example through ubiquitination of the negative regulator SMAD7 (MIM: 602932) and through direct binding to the E3 ubiquitin ligase SMURF2 (MIM: 605532). RLIM is important in the control of cell proliferation, in particular, by upregulating the TP53 (MIM: 191170) pathway and inhibiting c-Myc transcriptional activity via ubiquitination of MDM2 (MIM: 164785). Finally, RLIM is shown to regulate estrogen-responsive genes, through ubiquitination and phosphorylation of estrogen receptor alpha, and to have positive regulation of the TGF-beta family signaling pathway.[5,6] RLIM has been identified as a dose-dependent activator of X chromosome inactivation (XCI) in mouse embryonic stem cells (mESCs).[12] Subsequent studies using mESCs showed that RLIM controls XCI by targeting the XCI inhibitor Zfp42 (also known as Rex1 [MIM: 614572]) for proteasomal degradation.[13] RLIM protein functions also outside XCI in regulation of RNA polymerase III-dependent transcription.[14]

The impact of structural variants involving *RLIM* has not previously been reported. Here we describe 14 affected males from 9 families with a neurodevelopmental phenotype and overlapping X chromosomal duplications containing *RLIM*.

Through sharing of Australian case subjects and interrogation of entries in the NSW DECIPHER consortium, five Australian families were identified with males who had a neurodevelopmental phenotype and overlapping duplications on Xq13.2–13.3.[15] As *RLIM* was the only gene in the shortest region of overlap, we used the gene-oriented query "*RLIM*" to interrogate two publicly available repositories of clinical genetic variation in an attempt to find additional cases: (1) The Database of Chromosomal Imbalance and Phenotype in Humans using Ensembl Resources, DECIPHER[15] and (2) the public archive of interpretations of clinically relevant variants, ClinVar. Individual scientists were contacted for affected individuals/cases with *RLIM* containing duplications of less than 5 Mb in size and were asked for more clinical information where family consent was obtainable. Through these means, four additional families (families 6–9; Table 1) were identified with overlapping duplications. All families in the present cohort consented to publication of clinical data and, for seven out of the nine families, publication of clinical photographs, as per local ethics committee guidelines. Gene annotations of the extracted duplications refer to the genome build GRCh38/hg38.

Chromosomal microarray was performed as a diagnostic genetic test in all families with appropriate local consent, with details of the platform used by each diagnostic laboratory presented in Supplemental Note: Case reports. XCI studies were undertaken for families 1–5 and 7 (Table 1) using standard methodology.[16] FISH studies were performed for families 2 and 8 with a standard protocol using probes specific to the duplication and a control region (RP11-79C13 and DXZ1 at Xq13.3 and the ChrX centromere, respectively: Figure S1 for family 8).

To evaluate for the possibility of additional genomic lesions contributing to individual 1 (III:1)'s developmental and epileptic encephalopathy and individual 5 (III:1)'s more severe autism and developmental delay, whole-genome sequencing (WGS) was performed.[17] The WGS data were interrogated for rare sequence variants in brain-expressed genes identified under *de novo*, X-linked, compound heterozygous, and homozygous models. Structural variants were interrogated using the ClinSV pipeline.[18]

To further evaluate the effect of the Xq13 duplications in our cohort, lymphoblastoid cell lines (LCLs) were generated from affected males from Australian families 1–5 and a fibroblast cell line from the affected individual 2 (III:7) from family 2 using published methods.[19] The mRNA expression for three brain-expressed genes (*FTX* [MIM: 300936], *RLIM*, and *NEXMIF* [MIM: 300524]) in the duplicated region was examined in all cell lines. Expression of *SLC16A2* (MIM: 300095) was analyzed only in the fibroblast cell line as *SLC16A2* is not adequately expressed in LCLs. Protein levels of RLIM and known downstream interactors MDM2 and TP53 were assayed by western blot (see Supplemental Material and Methods).

The clinical characteristics of the 14 affected males in our cohort are presented in Table 2, pedigrees in Figure 1, and photographs in Figure 2. Detailed case reports for all individuals are available in the supplemental data

Table 1. Details of Genomic Findings from Chromosomal Testing Performed on Affected Individuals from Families 1–8

Family	1	2	3	4	5	6	7	8	9
Breakpoints of duplication	74,345,279–74,736,519	74,078,618–74,719,918	74,104,058–75,822,497	74,260,461–74,627,838	74,569,101–75,647,233	73,682,743–74,616,497	74,383,490–74,837,752	74,326,571–75,201,094	74,202,644–74,828,531
Protein-coding genes	*SLC16A2, RLIM,* (3′ end of *NEXMIF*)	*SLC16A2, RLIM*	*ZCCHC13, SLC16A2, RLIM, NEXMIF, ABCB7, UPRT, ZDHHC15, MAGEE2*	*ZCCHC13, SLC16A2, RLIM*	*RLIM, NEXMIF, ABCB7, UPRT, ZDHHC15*	*CHIC1, ZCCHC13, SLC16A2, RLIM*	*SLC16A2, RLIM, NEXMIF*	*SLC16A2, RLIM, NEXMIF, ABCB7, UPRT*	*SLC16A2, RLIM, NEXMIF*
Maternal XCI	100%	96%–100%	82%	100%	skewed	not done	moderately skewed	not done	not done
Other findings	Xq13.1 duplication (71,524,941–71,740,786) detected by WGS	Xq13.2 duplication (73,625,799–74,024,513)	none	paracentric inversion chromosome 11 assessed as non- pathogenic	within the duplicated region there is also a small deletion affecting *ABCB7*	none	none	127 kb deletion at 17q12 (37,440,306–37,566,809) assessed as variant of uncertain significance	16p13.11p12.3 duplication (14,945,367–16,813,003); 15q11.2 deletion* (18,471,716–20,731,389)

All genome coordinates relate to GRCh38/hg38 apart from family 9, 15q11.2del which relates to NCBI36/hg18 (*). Listed protein coding genes includes genes both partially and wholly in an individual's duplicated region. XCI refers to X-chromosome inactivation.

(Supplemental Note: Case reports). The most common neurocognitive phenotype was of mild ID, autism spectrum, social anxiety, disordered sleep, and hyperactivity. Most affected males were described as having a pleasant and happy behavioral profile. All required additional educational assistance: individual 3 (III:1) and individual 7 (III:1) were in specialist education in a high school with both aiming to work in hospitality. Individual 5 (III:1) had moderate global developmental delay, severe anxiety, and expressive and receptive language delay. He was attending an autism support class in a mainstream school. Individual 1 (III:1) had the most severe neurocognitive phenotype in the cohort, characterized by a severe drug-resistant epilepsy, profound ID, and movement disorder. He was nonverbal and non-ambulant. Seizures were experienced by two other individuals and neither required ongoing antiepileptic therapy. When assessed as a group, common distinctive facial features were apparent, including straight, medially flared eyebrows, short palpebral fissures, and flat midface (Figure 2). Other than mild joint hypermobility, particularly of the small joints, no consistent pattern of other systemic features was noted.

In all families the duplication was inherited from an unaffected heterozygous mother (Figure 1). Further segregation studies in relatives of families 3, 4, and 5 demonstrated absence of the duplication in samples from all six maternal grandparents, consistent with *de novo* maternal duplication events. In families 1 and 5, the duplication was *not* detected in the tested maternal male relatives of the proband with normal learning. In family 2, the duplication was present in three males over three generations, with segregation being consistent with X-linked recessive inheritance (Figure 1). In all tested carrier mothers, XCI was moderately (>80%) to severely (>95%) skewed, indicating presence of a variant of clinical significance on the X chromosome (Table 1). As shown in Table 1 (families 1–9), although the gene content of the duplicated regions varied among families, all included the entire *RLIM* gene. FISH data from families 2 and 8 did not reveal insertional duplications, making it likely that the duplications were in tandem (Figure S1: family 8; family 2 data not shown). Affected males from families 1 and 5 were further evaluated by WGS. All rare sequence variants in brain-expressed genes identified on analysis for *de novo*, X-linked, compound heterozygous or homozygous models are listed in Table S1; however, none met the ACMG criteria for (likely) pathogenicity.[20] No likely causative variants were identified on interrogation of the mitochondrial DNA. On analysis for structural variants, further delineation of complex structural events on the X chromosome was possible (Figures 3 and 4). For the affected male from family 1 (III:1), WGS revealed two adjacent X chromosomal duplications, separated by a region of normal copy number. One duplication was separated by a fragment/region from chromosome Xq13.1 and had the breakpoints 71,524,941–71,740,786 (hg38). It was 215 kb in size and included the protein coding genes *OGT* (MIM: 300255), *GCNA* (MIM: 300369), and *CXCR3* (MIM: 300574), as well as the 3′ non

Table 2. Clinical Features of Affected Individuals from Families 1–9

Individual	1 (III:1)	2 (III:7)	2 (II:4)	2 (IV:1)	3 (III:1)	4 (III:1)	4 (III:2)	5 (III:1)	6 (II:1)	7 (III:1)	8 (III:1)	9 (III:1)	9 (III:2)	9 (III:3)
Current age (years)	11	23	60	20	15	8	5	6	NR	16	9	11	5	3
Ethnicity	Australian	Australian	Australian	Australian	Australian	Australian	Australian	Australian	French	UK	USA	French	French	French
Gestation at birth	36 weeks	term	term	term	term	29 weeks	36 weeks	term	term	term	term	term	term	term
Prenatal complication	intra-uterine growth restriction	mild gestational hypertension	none	none	none	antenatal hemorrhage	threatened premature delivery	diet controlled gestational diabetes	none	none	antenatal hemorrhage	none	none	antenatal hemorrhage
Perinatal complication	none	congenital hip dysplasia	none	none	none	none	none	none	none	none	none	none	none	none
Birth weight	2.5 kg	3.6 kg	N/D	N/D	4.2 kg	1.5 kg	3.65 kg	N/D	3.2 kg	3.5 kg	3.43 kg	3.02 kg	3.25 kg	3.26 kg
Phenotype: ID	severe – profound ID	mild ID	mild ID	mild ID	mild ID	mild ID	mild ID	moderate ID	learning difficulties; speech delay	mild ID	mild ID	moderate ID	mild ID	speech delay
Phenotype: Seizures	developmental and epileptic encephalopathy	no	no	one possible afebrile seizure	prolonged febrile seizures	no	no	one possible afebrile seizure	no	no	no	no	no	no
Phenotype: ASD	some ASD features	some ASD features	no	no	ASD	ASD	some ASD features	level 3 ASD	no	some ASD feature	pervasive development disorder	no	no	no
Phenotype: other behavioral	no	aggression prior to dexamp hetamine	no	no	no	no	no concerns	anxiety, hyperarousal	no	challenging behaviors	mood swings	anxiety	no	no
Phenotype: other learning difficulties	no	ADHD	no	ADHD, dyslexia	ADHD	easily distracted	poor concentration and sustained attention	hyperactivity	hyperactivity	hyperactivity	no	easily distracted, poor concentration	no	no
Phenotype: sleep	no concerns	disordered sleep	no concerns	no concerns	disordered sleep initiation	disordered sleep initiation and maintenance	no concerns	disordered sleep initiation and maintenance	no concerns	no concerns	disordered sleep	disordered sleep initiation and maintenance	no	no
MRI	prominent CSF spaces	N/D	N/D	neuroepithelial cyst and white matter hyperintensities	normal	normal	N/D	normal	N/D	N/D	N/D	normal	N/D	N/D
Phenotype: musculoskeletal	hypotonic	congenital hip dysplasia, pes planus, metatarsus adductus	none	none	hypermobility fingers, wrist, flat feet, pes planus	hypotonia, easy fatigability	low muscle tone, small joint hypermobility	hypotonia, flexible small joints	none	hypotonia in infancy, restricted elbow extension	none	bilateral talipes equinovarus, pes planus	fifth finger clinodactyly	none

(*Continued on next page*)

Table 2. ***Continued***

Individual	1 (III:1)	2 (III:7)	2 (II:4)	2 (IV:1)	3 (III:1)	4 (III:1)	4 (III:2)	5 (III:1)	6 (II:1)	7 (III:1)	8 (III:1)	9 (III:1)	9 (III:2)	9 (III:3)
Phenotype: other non-neurological	none	idiopathic thrombo cytopenic purpura, hay fever, hyperacusis	none	childhood-onset hypothyroidism, asthma	asthma	myopia, hernia	none	recurrent ear infections	small ears; short fifth fingers	asthma, recurrent croup, eustachian ear tubes for OME	constipation	none	none	asthma
Current height (centile)	10^{th}	25^{th}–50^{th}	N/D	25^{th}–50^{th}	50^{th}–75^{th}	N/D	N/D	50^{th}–75^{th}	50^{th}	10^{th}–25^{th}	13^{th}	75^{th}–90^{th}	50^{th}	90^{th}
Current weight (centile)	$<2^{nd}$	50^{th}	N/D	90^{th}	75^{th}	N/D	N/D	25^{th}–50^{th}	25^{th}–50^{th}	75^{th}	6^{th}	90^{th}	75^{th}–90^{th}	75^{th}
Current head circumference (centile)	3^{th}–5^{th}	98^{th}	N/D	50^{th}	75^{th}	25^{th}	75^{th}–90^{th}	50^{th}	2^{nd}	25^{th}	25^{th}	50^{th}	25^{th}–50^{th}	50^{th}
Facial features	medially flared eyebrows, deep set relatively small eyes, straight eyebrows, thin upper lip	short palpebral fissures and medially flared eyebrows, flat midface	–	medially flared eyebrows, bilateral epicanthic folds, short palpebral fissures	high broad forehead, flat midface, medially flared eyebrows, short palpebral fissures	almond shaped eyes, flattened mid face	almond shaped eyes, up-slanting palpebral fissures, flattened mid face, epicanthic folds	–	–	ptosis, short palpebral fissures, straight eyebrows, posteriorly rotated ears	anterior hair whorl	high forehead, relatively short palpebral fissures, high arched eyebrows sparse laterally, flattened midface, prognathism	short palpebral fissures, medially flared eyebrows, flat midface	high broad forehead, protruding simple ears with anteverted lobes, eyebrows sparse laterally, bilateral epicanthic folds, short palpebral fissures, flattened midface

Abbreviations: N/D, no data; NR, not reported; OME, otitis media with effusion; ASD, autism spectrum disorder; CSF cerebrospinal fluid; ID, intellectual disability; ADHD, attention deficit hyperactivity disorder.

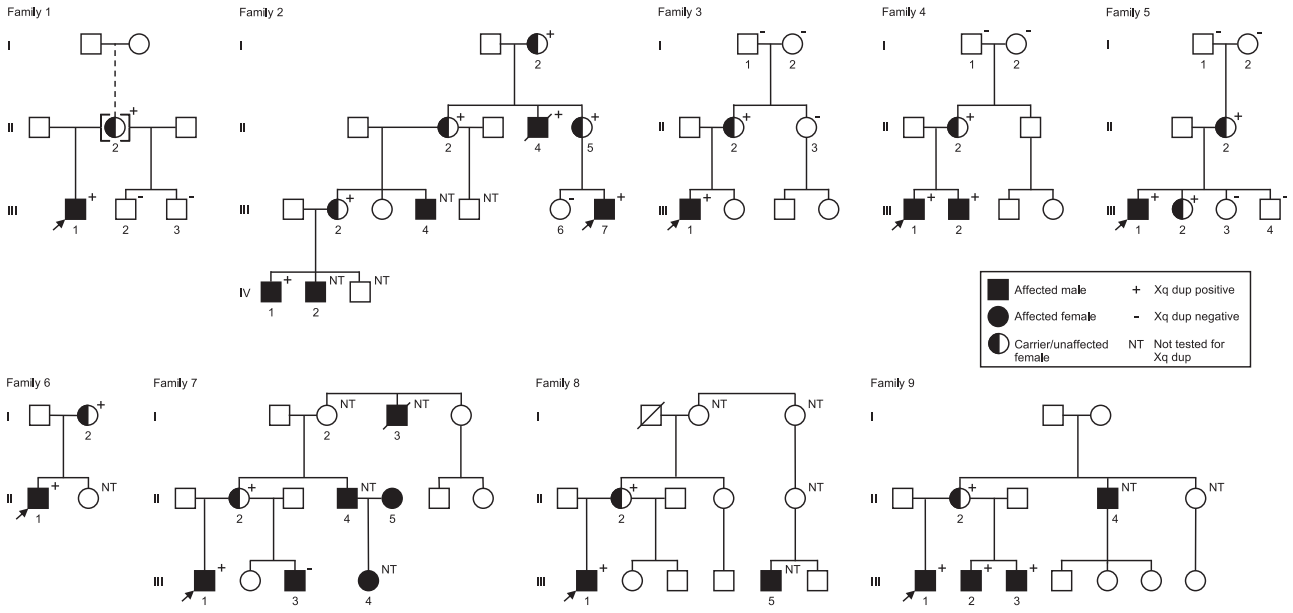

Figure 1. Pedigrees
Pedigrees of families with Xq13.2–13.3 duplication: affected males with neurodevelopmental disorder, filled boxes; unaffected carrier females, half-filled circles; tested individuals with Xq duplication are marked with a plus sign; tested individuals without Xq duplication are marked with a minus sign; individuals who have not been tested are denoted "NT;"

translated region of *TAF1* (MIM: 313650). The more distal duplication contained chromosomal material from Xq13.2q13.3. The breakpoints were refined to chrX: 74,345,279–74,736,519 (hg38), which included the 3′ region of *NEXMIF* (also known as *KIAA2022*) as well as *SLC16A2* and *RLIM*. The duplication was 391 kb in size. The duplicated segments are contiguous with one in inverted orientation to the other based on evidence from split read and discordant pairs (Figure 3). It was not possible to discern the insertion site of the fragment as the data (model I or model II) can be explained by two possible alignments. For individual 5 (III:1), data from read depth, split read, and discordant pairs were consistent with a simple tandem duplication in a male (Figure 4). Within the duplicated region there is also a small deletion affecting *ABCB7* (GenBank: NM_001271696, MIM: 300135). The deletion is predicted to remove exon 4 or create an intron retention which could lead to a frameshift and premature truncation. One intact copy of *ABCB7* was predicted to remain. The single exon deletion of *ABCD7* was not apparent on the original 60K ISCA oligonucleotide array.

RLIM expression was increased in all tested hemizygous male LCLs compared to four male control subjects and *FTX* expression was increased only in the males from families 2, 3, and 4 with this gene wholly or partially duplicated. *FTX* expression in families 1 and 5, i.e., individuals without *FTX* gene duplication, was similar to control subjects (Figure 5). *NEXMIF* expression varied greatly between affected male LCL samples irrespective of whether *NEXMIF* was included in their duplicated region. Large variation was also observed in the four male control samples, and also in an RNA sequencing dataset of 95 male control LCLs (Figure S3). *NEXMIF* expression appeared increased in the affected individual 2 (III:7)'s fibroblast sample as compared to five male control subjects, despite the gene not being duplicated in this individual (Figure 5). Given the negligible expression of *SLC16A2* in LCLs, its expression was interrogated only in individual 2 (III:7)'s fibroblast sample, which was not significantly different to control subjects. *RLIM* expression was also interrogated in LCLs from the mothers in families 1, 2, and 3 (Figure S2) and showed that expression was not significantly different from control subjects, consistent with their skewed X chromosome inactivation status and normal clinical presentation.

We evaluated the functional impact of the Xq13 duplications by determining the protein levels of RLIM and its known downstream interacting partners MDM2 and TP53 by western blot assay (Figure 6). Compared to control subjects, the affected LCLs from families 1–5 (where cell lines were available) showed significantly increased RLIM and moderately yet consistently across all affected individuals tested, reduced levels of the RLIM E3 ligase target MDM2. However, the levels of MDM2's target TP53 seemed unaltered. We also examined protein expression levels in two male LCLs with the pathogenic *RLIM* missense variant (GenBank: NM_016120.4 [*RLIM*]; c.1093C>T [p.Arg365Cys]) that had previously been demonstrated to result in retained, if not possibly increased, ubiquitination.[8] The missense variants were associated with significantly reduced RLIM protein levels, a small decrease in MDM2 levels compared to wild type, and no discernable difference in TP53 levels (Figure 6).

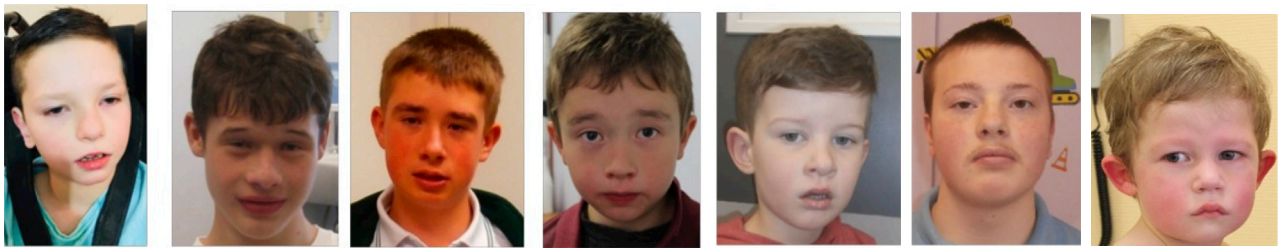

Figure 2. Photographs
Facial features of males with Xq13.2–13.3 duplications where families consented to sharing photographs. Common distinctive facial features include straight, medially flared eyebrows, short palpebral fissures, and flat midface.

On aggregate the overlapping similarity of clinical, genomic, and expression study results from this patient cohort supports the hypothesis that *RLIM* is a dosage-sensitive gene and that increased protein levels arising from duplications are associated with neurocognitive abnormalities. Consistent with this hypothesis, Frints and colleagues and Bustos and colleagues,[5,6] by examining the functional consequence of missense variants affecting different domains of the RLIM protein, demonstrated that some sequence variants were associated with increased ubiquitin ligase activity, whereas others had reduced activity. Based on multiple lines of evidence, the authors concluded these missense variants are likely to represent loss-of-function alleles.[5] Their findings are also supportive of *RLIM* being a dosage-sensitive gene, where primarily decreased expression of *RLIM* may lead to complex downstream modifications in pathways important for neuronal development and function.[5,6] Several other E3 ubiquitin ligase genes have been demonstrated to have an exquisite dosage sensitivity, whereby both reduction and increase in gene dosage is associated with a neurodevelopmental phenotype.[21–23] Our own expression data from LCLs in a control population (Figure S3) shows very tight *RLIM* expression values, also supporting the observation that RLIM might be under tight dosage regulation.

Many conditions resulting from increased or decreased expression of a dosage-sensitive gene result in both, some phenotypic similarities and distinctions. For example, Smith-Magenis syndrome (SMS [MIM: 182290]) caused by deletion of 17p11.2 region or haploinsufficiency of the critical gene *RAI1* (MIM: 607642) has many phenotypic similarities to, but also some differences from, Potocki-Lupski syndrome (PTLS [MIM: 610883]). caused by duplication or triplication of the 17p11.2 region.[24] The cohort of individuals with duplications including *RLIM* described here share many phenotypic features with individuals from families with *RLIM* single-nucleotide variants, including autism spectrum, ID, ADHD, and behavioral issues. However, they lack the more severe multiple congenital malformations which are described in affected individuals with deleterious variants in the RING finger domain: these variants most severely affect the ability of RLIM to ubiquitinate substrate(s).[5] Such severe effects may be selectively due to single-nucleotide damaging variants predicted to result in severe RLIM LoF.[5]

It is possible that the structural variants identified in our cohort have a more distant, in *cis*, effect on X chromosome gene expression or that other genes in this region may have a modifying impact on the phenotype, also depending on the size of the duplication. We have not tested these possibilities. We list all the genes included in the differently sized duplications in our cohort in Table S2 and discuss three genes in more detail here: *SLC16A2* and *NEXMIF* (expressed in brain and associated with clinical phenotypes)[25,26] and *FTX* (implicated in a neurological phenotype in animal studies).[27]

Several (but not all) duplications included the whole of *SLC16A2*, a gene in which LoF and missense variants cause Allan-Herndon-Dudley syndrome (AHDS [MIM: 300523]). AHDS is characterized by severe infantile hypotonia, reduced muscle mass, progressive spastic quadriplegia and dystonia/athetoid movement disorder, and an increased risk of seizures[25] due to decreased access of thyroid hormone to the developing brain.[28] All individuals with AHDS have pathognomonic changes in thyroid function tests (T3, reverse T3, thyroxine, and TSH concentrations). However, all tested males with the *SLC16A2* duplication in our cohort (individuals from families 1, 2, 4, and 7) did not have this pattern of thyroid function changes and *SLC16A2* expression was not significantly increased in fibroblasts in the one affected male (individual III:7 from family 2) where this cell line was available for testing, compared to control subjects (Figure 5). We could not obtain consent for generating fibroblasts for other affected individuals in the cohort.

We considered the possible role of *FTX* and *NEXMIF* overexpression. Although no human neurocognitive phenotype has been described in association with variants in the long non-coding gene *FTX*, a recent report shows that *Ftx* targeted deletion causes eye abnormalities in a subset of female mice and in a rat model of temporal lobe epilepsy, *Ftx* levels were reduced, while overexpression of *Ftx* reduced seizure activity and inhibited hippocampal apoptosis.[27] There is

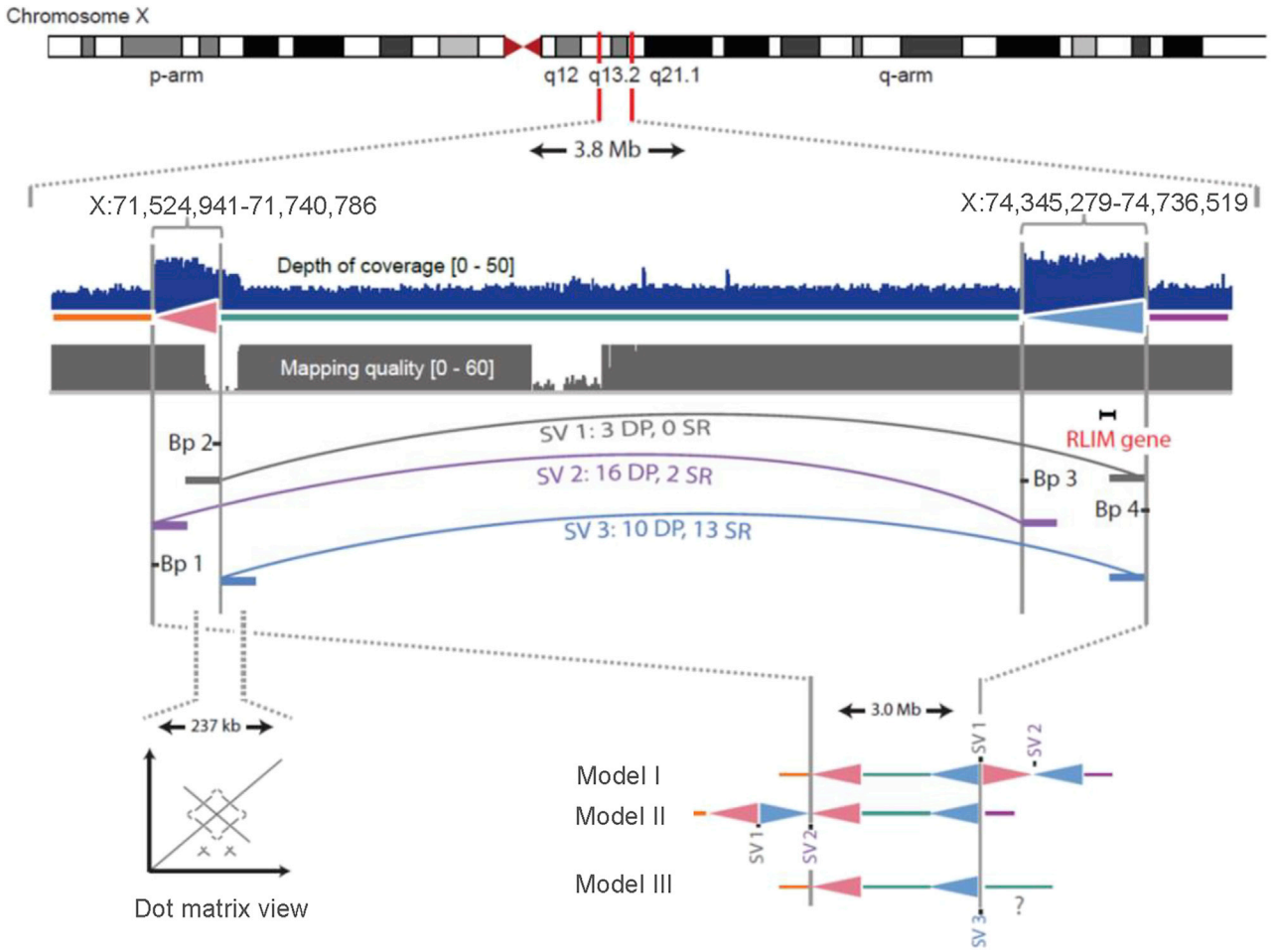

Figure 3. Duplication of *RLIM* Caused by Structural Variants, Revealed by WGS in the Male Probands from Family 1
This panel demonstrates the location of the two duplications relative to the X chromosome and *RLIM*, i.e., Xq13.1 (red triangle) and Xq13.2–13.3 (blue triangle) in the proband from family 1. The depth of coverage is shown in blue and the phred scaled read mapping quality in gray ($Q = -10 \log_{10} * P$, Q of 30 corresponds to 1 misaligned reads in 1,000). The structural variants (SVs) and their supporting discordant pairs (DP) and split reads (SR) are shown. The WGS data indicate the existence of four breakpoints (labeled Bp1–4) and 3 structural variants (SV1–3). Also shown is a dot matrix view of genome sequence surrounding breakpoint 2 (Bp2) aligned to itself, showing a palindromic sequence that could cause DP and SR reads to misalign. As a result, SV1 and SV3 could represent a single SV. Alongside is shown models of the rearrangement considering depth of coverage change, discordant pairs, and split reads. Model I and II are equally plausible and only involve SV1 and SV2. A model involving SV3 is not plausible as it would require the middle section between both duplications to also be duplicated (model III), which contradicts the observed depth of coverage. The sequencing reads of SV3 at Bp2 are most likely wrongly mapped due to the palindrome and should instead map upstream of Bp2, which then provides further supporting evidence for SV1, thus SV1 and SV2 being the only real SV in this region. Breakpoints are provided in hg38.

growing evidence that *FTX* is important in the control of XCI,[29,30] and abnormalities of *FTX* expression have also been reported in various cancer tissues as well as in areas of ischemia.[31] Interestingly *FTX* expression was significantly increased in individuals from families 2, 3, and 4 with *FTX* duplication. However, *FTX* is not duplicated in all affected individuals in this cohort. While there is currently no clear evidence that an increased dosage of *FTX* would cause a neurocognitive phenotype in males, it is conceivable that *FTX* overexpression might modulate the phenotype given that the phenotype is very similar in affected individuals from families 2, 3, and 4 and milder than for individuals from families 1 and 5.

Affected individuals from families 3 and 5 carry a full-length *NEXMIF*, previously known as *KIAA2022*, duplication, whereas the breakpoint in the affected male in family 1 (III:1) is located within the 3′ UTR (*NEXMIF* is on the antisense strand). Although *NEXMIF* is not included in all individuals with duplications in our cohort, its potential role in the phenotype of individuals from families 1, 3, and 5 was considered further. LoF variants in *NEXMIF* are established as the cause of a typically severe neurocognitive phenotype (mental retardation, X-linked 98 [MIM: 300912]). In affected males, the phenotype is characterized by intellectual disability, typically severe to profound, with common comorbidities of autism and behavioral disorders, epilepsy, infantile hypotonia evolving to spasticity, gastrointestinal issues, strabismus, and stereotypical movements.[26] Dysmorphic features have also been noted but there is not a clearly distinctive facial gestalt. Pathogenic

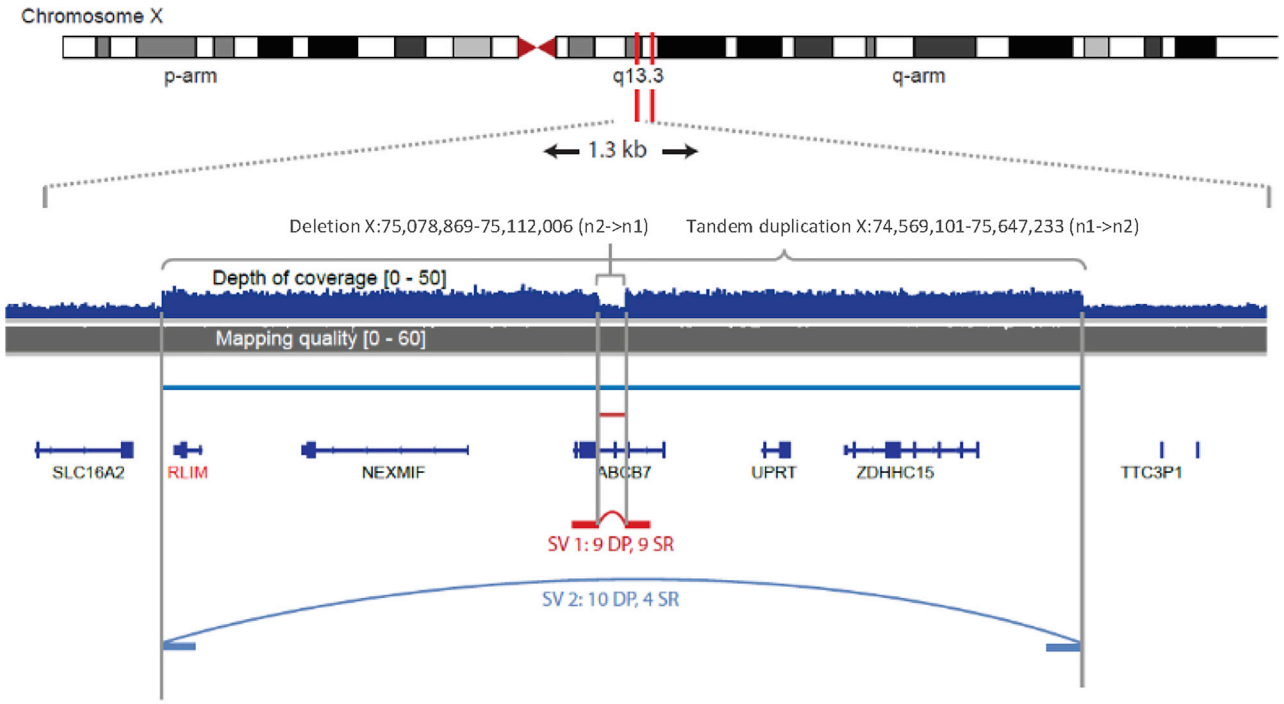

Figure 4. Duplication of *RLIM* Caused by Structural Variants, Revealed by WGS in the Male Probands from Family 5
This panel demonstrates duplication relative to the X chromosome and *RLIM* in the proband from family 5. Evidence from split reads is shown, consistent with the duplication being a simple tandem duplication, which contains a small deletion within *ABCB7*. Breakpoints are provided in hg38.

variants either occur *de novo* or are inherited from an asymptomatic carrier mother with highly skewed X chromosome inactivation. *De novo* loss of one allele of *NEXMIF* in females is characterized by moderate-severe ID, infantile hypotonia, a seizure disorder that can be consistent with a developmental and epileptic encephalopathy, autistic features, and progressive spasticity and movement disorder.[32–38] X chromosome inactivation in these females is usually random, and the resulting cellular mosaicism likely contributes to the pathology.[34,39] *NEXMIF* plays important roles in the control of neuronal migration and morphogenesis.[37,40] Several groups have described individuals with this phenotype and reduced *NEXMIF* expression resulting from structural variations including partial[37] and whole[41] gene duplications and inversions and translocations with breakpoints within *NEXMIF*.[37,42,43] Charzewska and colleagues[41] reported a multi-generational family with five affected males with moderate-severe ID and increased chance of seizures, in whom the whole of *NEXMIF* was duplicated. Expression of *NEXMIF* was reduced by ~60% in LCLs and by ~90% in fibroblasts using RT-qPCR, which the authors suggested could be due to a duplication disrupting association with non-coding regulatory regions; however, the actual experimental data were not shown.[41] In our cohort, the effect of *NEXMIF* duplication was, at first sight, unclear, due to large variation in expression levels in all LCL samples, including controls (Figure 5), and we were unable to reconcile the effect of genomic dosage of *NEXMIF* on its mRNA level. We therefore decided to investigate further by interrogating *NEXMIF* mRNA expression in LCL in a larger control population available to our laboratory (n = 95) and which clearly shows that *NEXMIF* mRNA expression varies widely in the population (Figure S3). We therefore recommend careful interpretation of the significance of any alteration involving *NEXMIF* mRNA in at least LCLs.

The more severe phenotype observed in the affected male from family 1 (III:1) is not yet fully explained. It is possible that an additional unidentified genomic lesion is contributing to a potentially blended phenotype. It could also be possible that the complex structural variation unveiled by WGS affects the 3D genomic configuration influencing the expression or function of other genes located in this region.

The true incidence of Xq13.2–13.3 duplications in males with intellectual disability is currently unknown, but it is striking that we have detected four individuals under 16 years old with overlapping duplications from one Australian state (NSW: affected individuals from families 1, 3, and 4). This suggests that copy number duplications in this X chromosome region may be relatively frequent but to date have been underidentified and/or underreported due to the relatively mild neurodevelopmental features and inherent difficulty attributing pathogenicity to chromosomal duplications overall.

In summary, the evidence presented here supports the notion that duplications at the Xq13.2–13.3 locus result in a syndromic neurocognitive condition in hemizygous males. The phenotype is most typically of mild ID, some

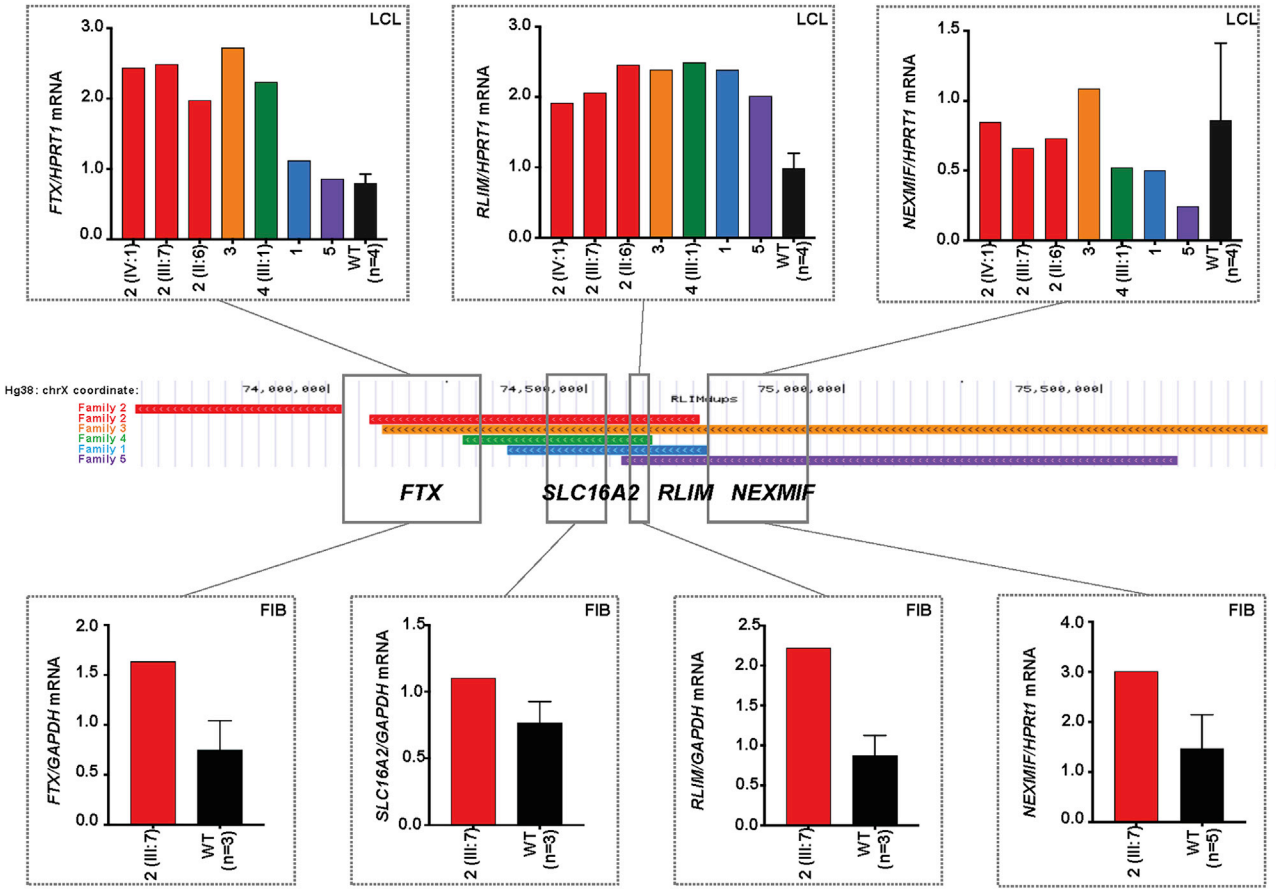

Figure 5. Gene Expression Studies
RT-qPCR analysis of *FTX*, *RLIM*, and *NEXMIF* expression in LCLs from the affected males from families 1–5 (upper graphs) and RT-qPCR analysis of *FTX*, *SLC16A2*, *RLIM*, and *NEXMIF* expression in fibroblasts (FIB) from individual 2 (III:7) from family 2 (lower graphs), with a graphic depiction of the duplicated region in each family tested. Samples were run in triplicate and mean gene expression was normalized to mean expression of either *HPRT1* or *GAPDH*. WT male data is presented as mean ± SD (error bars).

features on the autistic spectrum, hyperactivity, and subtly distinctive facial features including short palpebral fissures and a relatively flat midface. Our data suggest that the most likely gene for the core phenotype is *RLIM* because *RLIM* is the only fully duplicated gene in all subjects (Table 1) and because the extra copy of *RLIM* leads to increased mRNA as well as RLIM protein levels in cells of all tested affected males (Figures 5 and 6). In addition, many roles played by RLIM including E3 ubiquitin ligation and transcriptional regulation make it a plausible dosage-sensitive gene. However, we cannot exclude the possibility of phenotype-modifying effects of other *RLIM*-flanking genes, particularly *FTX*, *SLC16A2*, and *NEXMIF*. Confirmation of these findings in a larger clinical cohort will be required to clarify the significance, genotypic-phenotypic spectrum, and reproductive counseling implications of this previously undescribed X chromosome-linked condition. This study, along with the studies describing phenotypes associated with duplications of *HUWE1*, *STAG2* (MIM: 300826), and *MECP2* (MIM: 300005) and the Xq25q26 duplication syndrome containing both *GPC3* (MIM: 300037) and *IGSF1* (MIM: 300137)[22,44–47] supports the hypothesis that X chromosome duplications involving highly constrained and known ID genes are worthy of further investigations.

Data and Code Availability

The accession number(s) for the copy number variants (CNV) sequences reported in this paper are DECIPHER: 349687, 345319, 345223, 368481, 251339, 262593, and 368494 and CLINVAR: VCV000060333.1 and VCV000154937. Next generation sequencing data has not been deposited in a public repository because of consent and IRB/Human Research Ethics Committee restrictions on patient data, but the data are available from the corresponding author on request.

Supplemental Data

Supplemental Data can be found online at https://doi.org/10.1016/j.ajhg.2020.10.005.

Acknowledgments

This study makes use of data generated by the DECIPHER community. A full list of contributing centers is available online and via

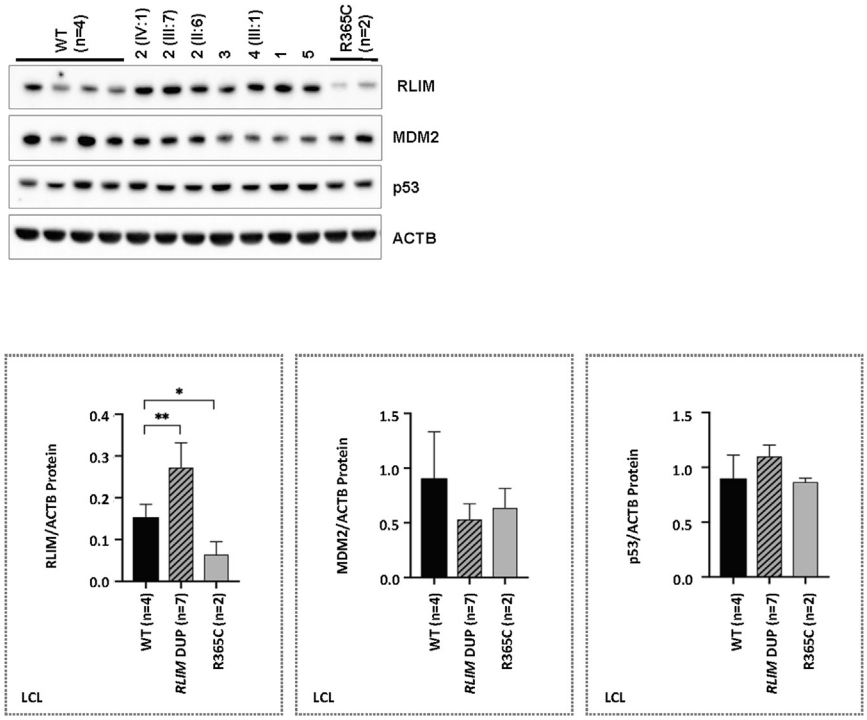

Figure 6. Protein Expression Studies
Western blots of LCL lysates probed for RLIM and its downstream targets MDM2 and TP53. ACTB was used as a loading control. RLIM, MDM2, and TP53 western blot signals were quantified using Image Lab software (Bio-Rad) and their normalized values relative to ACTB signal intensity were plotted. *p = 0.029 and **p = 0.006, using a two-tailed unpaired t test. Control subjects were four individuals with wild-type RLIM, "RLIM dup" were 7 individuals with chromosomal duplications from the current cohort with all of *RLIM* duplicated, and "R365C" were two brothers with a previously reported missense variant in *RLIM* p.Arg365Cys. The data are presented as mean ± SD (error bars).

email from decipher@sanger.ac.uk. Funding for the project was provided by the Wellcome Trust. We thank Associate Professor Erin Riggs from the Autism & Developmental Medicine Institute, Geisinger, for her assistance in linking ISCA consortium data to the relevant diagnostic team. We thank la Biobanque de Picardie (BB-0033-00017). This study was supported by National Health and Medical Research Council of Australia grants GNT11149630 to E.P. and APP1155224 and 1091593 and Channel 7 Children's Research Foundation to J.G.

Declaration of Interests

The authors declare no competing interests.

Received: May 22, 2020
Accepted: October 13, 2020
Published: November 6, 2020

Web Resources

CLINSV Github, https://github.com/KCCG/ClinSV
CLINVAR (accessed May 2018), https://www.ncbi.nlm.nih.gov/clinvar
DECIPHER (accessed May 2018), https://decipher.sanger.ac.uk
GenBank, https://www.ncbi.nlm.nih.gov/genbank/
GnomAD-SV, https://gnomad.broadinstitute.org/
OMIM, https://omim.org/
Pubmed, https://pubmed.ncbi.nlm.nih.gov

References

1. Tzschach, A., Grasshoff, U., Beck-Woedl, S., Dufke, C., Bauer, C., Kehrer, M., Evers, C., Moog, U., Oehl-Jaschkowitz, B., Di Donato, N., et al. (2015). Next-generation sequencing in X-linked intellectual disability. Eur. J. Hum. Genet. *23*, 1513–1518.
2. Turner, G., Boyle, J., Partington, M.W., Kerr, B., Raymond, F.L., and Gécz, J. (2008). Restoring reproductive confidence in families with X-linked mental retardation by finding the causal mutation. Clin. Genet. *73*, 188–190.
3. Tønne, E., Holdhus, R., Stansberg, C., Stray-Pedersen, A., Petersen, K., Brunner, H.G., Gilissen, C., Hoischen, A., Prescott, T., Steen, V.M., and Fiskerstrand, T. (2015). Syndromic X-linked intellectual disability segregating with a missense variant in RLIM. Eur. J. Hum. Genet. *23*, 1652–1656.
4. Hu, H., Haas, S.A., Chelly, J., Van Esch, H., Raynaud, M., de Brouwer, A.P., Weinert, S., Froyen, G., Frints, S.G., Laumonnier, F., et al. (2016). X-exome sequencing of 405 unresolved families identifies seven novel intellectual disability genes. Mol. Psychiatry *21*, 133–148.
5. Frints, S.G.M., Ozanturk, A., Rodríguez Criado, G., Grasshoff, U., de Hoon, B., Field, M., Manouvrier-Hanu, S., E Hickey, S., Kammoun, M., Gripp, K.W., et al. (2019). Pathogenic variants in E3 ubiquitin ligase RLIM/RNF12 lead to a syndromic X-linked intellectual disability and behavior disorder. Mol. Psychiatry *24*, 1748–1768.
6. Bustos, F., Segarra-Fas, A., Chaugule, V.K., Brandenburg, L., Branigan, E., Toth, R., Macartney, T., Knebel, A., Hay, R.T., Walden, H., and Findlay, G.M. (2018). RNF12 X-Linked Intellectual Disability Mutations Disrupt E3 Ligase Activity and Neural Differentiation. Cell Rep. *23*, 1599–1611.
7. Abraham, J.R., Barnard, J., Wang, H., Noritz, G.H., Yeganeh, M., Buhas, D., and Natowicz, M.R. (2019). Proteomic investigations of human HERC2 mutants: Insights into the pathobiology of a neurodevelopmental disorder. Biochem. Biophys. Res. Commun. *512*, 421–427.
8. Tarpey, P.S., Raymond, F.L., O'Meara, S., Edkins, S., Teague, J., Butler, A., Dicks, E., Stevens, C., Tofts, C., Avis, T., et al. (2007). Mutations in CUL4B, which encodes a ubiquitin E3 ligase

subunit, cause an X-linked mental retardation syndrome associated with aggressive outbursts, seizures, relative macrocephaly, central obesity, hypogonadism, pes cavus, and tremor. Am. J. Hum. Genet. *80*, 345–352.
9. Moortgat, S., Berland, S., Aukrust, I., Maystadt, I., Baker, L., Benoit, V., Caro-Llopis, A., Cooper, N.S., Debray, F.G., Faivre, L., et al. (2018). HUWE1 variants cause dominant X-linked intellectual disability: a clinical study of 21 patients. Eur. J. Hum. Genet. *26*, 64–74.
10. Zhang, J., Gambin, T., Yuan, B., Szafranski, P., Rosenfeld, J.A., Balwi, M.A., Alswaid, A., Al-Gazali, L., Shamsi, A.M.A., Komara, M., et al. (2017). Haploinsufficiency of the E3 ubiquitin-protein ligase gene TRIP12 causes intellectual disability with or without autism spectrum disorders, speech delay, and dysmorphic features. Hum. Genet. *136*, 377–386.
11. Kishino, T., Lalande, M., and Wagstaff, J. (1997). UBE3A/E6-AP mutations cause Angelman syndrome. Nat. Genet. *15*, 70–73.
12. Jonkers, I., Barakat, T.S., Achame, E.M., Monkhorst, K., Kenter, A., Rentmeester, E., Grosveld, F., Grootegoed, J.A., and Gribnau, J. (2009). RNF12 is an X-Encoded dose-dependent activator of X chromosome inactivation. Cell *139*, 999–1011.
13. Gontan, C., Achame, E.M., Demmers, J., Barakat, T.S., Rentmeester, E., van IJcken, W., Grootegoed, J.A., and Gribnau, J. (2012). RNF12 initiates X-chromosome inactivation by targeting REX1 for degradation. Nature *485*, 386–390.
14. Wang, F., Zhao, K., Yu, S., Xu, A., Han, W., and Mei, Y. (2019). RNF12 catalyzes BRF1 ubiquitination and regulates RNA polymerase III-dependent transcription. J. Biol. Chem. *294*, 130–141.
15. Firth, H.V., Richards, S.M., Bevan, A.P., Clayton, S., Corpas, M., Rajan, D., Van Vooren, S., Moreau, Y., Pettett, R.M., and Carter, N.P. (2009). DECIPHER: Database of Chromosomal Imbalance and Phenotype in Humans Using Ensembl Resources. Am. J. Hum. Genet. *84*, 524–533.
16. Allen, R.C., Zoghbi, H.Y., Moseley, A.B., Rosenblatt, H.M., and Belmont, J.W. (1992). Methylation of HpaII and HhaI sites near the polymorphic CAG repeat in the human androgen-receptor gene correlates with X chromosome inactivation. Am. J. Hum. Genet. *51*, 1229–1239.
17. Palmer, E.E., Hong, S., Al Zahrani, F., Hashem, M.O., Aleisa, F.A., Ahmed, H.M.J., Kandula, T., Macintosh, R., Minoche, A.E., Puttick, C., et al. (2019). De Novo Variants Disrupting the HX Repeat Motif of ATN1 Cause a Recognizable Non-Progressive Neurocognitive Syndrome. Am. J. Hum. Genet. *104*, 542–552.
18. Minoche, A.E., Lundie, B., Peters, G.B., Ohnesorg, T., Pinese, M., Thomas, D.M., Zankl, A., Roscioli, T., Schonrock, N., Kummerfeld, S., Burnett, L., Dinger, M.E., and Cowley, M.J. (2020). ClinSV: Clinical grade structural and copy number variant detection from whole genome sequencing data. medRxiv, 2020.06.30.20143453.
19. Vangipuram, M., Ting, D., Kim, S., Diaz, R., and Schüle, B. (2013). Skin punch biopsy explant culture for derivation of primary human fibroblasts. J. Vis. Exp. (77), e3779.
20. Richards, S., Aziz, N., Bale, S., Bick, D., Das, S., Gastier-Foster, J., Grody, W.W., Hegde, M., Lyon, E., Spector, E., et al.; ACMG Laboratory Quality Assurance Committee (2015). Standards and guidelines for the interpretation of sequence variants: a joint consensus recommendation of the American College of Medical Genetics and Genomics and the Association for Molecular Pathology. Genet. Med. *17*, 405–424.
21. Froyen, G., Belet, S., Martinez, F., Santos-Rebouças, C.B., Declercq, M., Verbeeck, J., Donckers, L., Berland, S., Mayo, S., Rosello, M., et al. (2012). Copy-number gains of HUWE1 due to replication- and recombination-based rearrangements. Am. J. Hum. Genet. *91*, 252–264.
22. Froyen, G., Corbett, M., Vandewalle, J., Jarvela, I., Lawrence, O., Meldrum, C., Bauters, M., Govaerts, K., Vandeleur, L., Van Esch, H., et al. (2008). Submicroscopic duplications of the hydroxysteroid dehydrogenase HSD17B10 and the E3 ubiquitin ligase HUWE1 are associated with mental retardation. Am. J. Hum. Genet. *82*, 432–443.
23. Copping, N.A., Christian, S.G.B., Ritter, D.J., Islam, M.S., Buscher, N., Zolkowska, D., Pride, M.C., Berg, E.L., LaSalle, J.M., Ellegood, J., et al. (2017). Neuronal overexpression of Ube3a isoform 2 causes behavioral impairments and neuroanatomical pathology relevant to 15q11.2-q13.3 duplication syndrome. Hum. Mol. Genet. *26*, 3995–4010.
24. Neira-Fresneda, J., and Potocki, L. (2015). Neurodevelopmental Disorders Associated with Abnormal Gene Dosage: Smith-Magenis and Potocki-Lupski Syndromes. J. Pediatr. Genet. *4*, 159–167.
25. Schwartz, C.E., and Stevenson, R.E. (2007). The MCT8 thyroid hormone transporter and Allan-Herndon-Dudley syndrome. Best Pract. Res. Clin. Endocrinol. Metab. *21*, 307–321.
26. Lorenzo, M., Stolte-Dijkstra, I., van Rheenen, P., Smith, R.G., Scheers, T., and Walia, J.S. (2018). Clinical spectrum of KIAA2022 pathogenic variants in males: Case report of two boys with KIAA2022 pathogenic variants and review of the literature. Am. J. Med. Genet. A. *176*, 1455–1462.
27. Li, X., Giri, V., Cui, Y., Yin, M., Xian, Z., and Li, J. (2019). LncRNA FTX inhibits hippocampal neuron apoptosis by regulating miR-21-5p/SOX7 axis in a rat model of temporal lobe epilepsy. Biochem. Biophys. Res. Commun. *512*, 79–86.
28. Dumitrescu, A.M., Liao, X.H., Best, T.B., Brockmann, K., and Refetoff, S. (2004). A novel syndrome combining thyroid and neurological abnormalities is associated with mutations in a monocarboxylate transporter gene. Am. J. Hum. Genet. *74*, 168–175.
29. Furlan, G., Gutierrez Hernandez, N., Huret, C., Galupa, R., van Bemmel, J.G., Romito, A., Heard, E., Morey, C., and Rougeulle, C. (2018). The Ftx Noncoding Locus Controls X Chromosome Inactivation Independently of Its RNA Products. Mol. Cell *70*, 462–472.e8.
30. Hosoi, Y., Soma, M., Shiura, H., Sado, T., Hasuwa, H., Abe, K., Kohda, T., Ishino, F., and Kobayashi, S. (2018). Female mice lacking Ftx lncRNA exhibit impaired X-chromosome inactivation and a microphthalmia-like phenotype. Nat. Commun. *9*, 3829.
31. Long, B., Li, N., Xu, X.X., Li, X.X., Xu, X.J., Guo, D., Zhang, D., Wu, Z.H., and Zhang, S.Y. (2018). Long noncoding RNA FTX regulates cardiomyocyte apoptosis by targeting miR-29b-1-5p and Bcl2l2. Biochem. Biophys. Res. Commun. *495*, 312–318.
32. Samanta, D., and Willis, E. (2020). KIAA2022-related disorders can cause Jeavons (eyelid myoclonia with absence) syndrome. Acta Neurol. Belg. *120*, 205–207.
33. Webster, R., Cho, M.T., Retterer, K., Millan, F., Nowak, C., Douglas, J., Ahmad, A., Raymond, G.V., Johnson, M.R., Pujol, A., et al. (2017). De novo loss of function mutations in KIAA2022 are associated with epilepsy and neurodevelopmental delay in females. Clin. Genet. *91*, 756–763.
34. de Lange, I.M., Helbig, K.L., Weckhuysen, S., Møller, R.S., Velinov, M., Dolzhanskaya, N., Marsh, E., Helbig, I., Devinsky,

O., Tang, S., et al.; EuroEPINOMICS-RES MAE working group (2016). De novo mutations of KIAA2022 in females cause intellectual disability and intractable epilepsy. J. Med. Genet. *53*, 850–858.
35. Farach, L.S., and Northrup, H. (2016). KIAA2022 nonsense mutation in a symptomatic female. Am. J. Med. Genet. A. *170*, 703–706.
36. Kuroda, Y., Ohashi, I., Naruto, T., Ida, K., Enomoto, Y., Saito, T., Nagai, J., Wada, T., and Kurosawa, K. (2015). Delineation of the KIAA2022 mutation phenotype: two patients with X-linked intellectual disability and distinctive features. Am. J. Med. Genet. A. *167*, 1349–1353.
37. Van Maldergem, L., Hou, Q., Kalscheuer, V.M., Rio, M., Doco-Fenzy, M., Medeira, A., de Brouwer, A.P., Cabrol, C., Haas, S.A., Cacciagli, P., et al. (2013). Loss of function of KIAA2022 causes mild to severe intellectual disability with an autism spectrum disorder and impairs neurite outgrowth. Hum. Mol. Genet. *22*, 3306–3314.
38. Palmer, E.E., Schofield, D., Shrestha, R., Kandula, T., Macintosh, R., Lawson, J.A., Andrews, I., Sampaio, H., Johnson, A.M., Farrar, M.A., et al. (2018). Integrating exome sequencing into a diagnostic pathway for epileptic encephalopathy: Evidence of clinical utility and cost effectiveness. Mol. Genet. Genomic Med. *6*, 186–199.
39. Tukiainen, T., Villani, A.C., Yen, A., Rivas, M.A., Marshall, J.L., Satija, R., Aguirre, M., Gauthier, L., Fleharty, M., Kirby, A., et al.; GTEx Consortium; Laboratory, Data Analysis &Coordinating Center (LDACC)—Analysis Working Group; Statistical Methods groups—Analysis Working Group; Enhancing GTEx (eGTEx) groups; NIH Common Fund; NIH/NCI; NIH/NHGRI; NIH/NIMH; NIH/NIDA; Biospecimen Collection Source Site—NDRI; Biospecimen Collection Source Site—RPCI; Biospecimen Core Resource—VARI; Brain Bank Repository—University of Miami Brain Endowment Bank; Leidos Biomedical—Project Management; ELSI Study; Genome Browser Data Integration &Visualization—EBI; and Genome Browser Data Integration &Visualization—UCSC Genomics Institute, University of California Santa Cruz (2017). Landscape of X chromosome inactivation across human tissues. Nature *550*, 244–248.
40. Gilbert, J., and Man, H.Y. (2016). The X-Linked Autism Protein KIAA2022/KIDLIA Regulates Neurite Outgrowth via N-Cadherin and δ-Catenin Signaling. eNeuro *3*, 3.
41. Charzewska, A., Rzońca, S., Janeczko, M., Nawara, M., Smyk, M., Bal, J., and Hoffman-Zacharska, D. (2015). A duplication of the whole KIAA2022 gene validates the gene role in the pathogenesis of intellectual disability and autism. Clin. Genet. *88*, 297–299.
42. Cantagrel, V., Lossi, A.M., Boulanger, S., Depetris, D., Mattei, M.G., Gecz, J., Schwartz, C.E., Van Maldergem, L., and Villard, L. (2004). Disruption of a new X linked gene highly expressed in brain in a family with two mentally retarded males. J. Med. Genet. *41*, 736–742.
43. Moysés-Oliveira, M., Guilherme, R.S., Meloni, V.A., Di Battista, A., de Mello, C.B., Bragagnolo, S., Moretti-Ferreira, D., Kosyakova, N., Liehr, T., Carvalheira, G.M., and Melaragno, M.I. (2015). X-linked intellectual disability related genes disrupted by balanced X-autosome translocations. Am. J. Med. Genet. B. Neuropsychiatr. Genet. *168*, 669–677.
44. Kumar, R., Corbett, M.A., Van Bon, B.W., Gardner, A., Woenig, J.A., Jolly, L.A., Douglas, E., Friend, K., Tan, C., Van Esch, H., et al. (2015). Increased STAG2 dosage defines a novel cohesinopathy with intellectual disability and behavioral problems. Hum. Mol. Genet. *24*, 7171–7181.
45. Van Esch, H., Bauters, M., Ignatius, J., Jansen, M., Raynaud, M., Hollanders, K., Lugtenberg, D., Bienvenu, T., Jensen, L.R., Gecz, J., et al. (2005). Duplication of the MECP2 region is a frequent cause of severe mental retardation and progressive neurological symptoms in males. Am. J. Hum. Genet. *77*, 442–453.
46. Møller, R.S., Jensen, L.R., Maas, S.M., Filmus, J., Capurro, M., Hansen, C., Marcelis, C.L., Ravn, K., Andrieux, J., Mathieu, M., et al. (2014). X-linked congenital ptosis and associated intellectual disability, short stature, microcephaly, cleft palate, digital and genital abnormalities define novel Xq25q26 duplication syndrome. Hum. Genet. *133*, 625–638.
47. Herriges, J.C., Arch, E.M., Burgio, P.A., Baldwin, E.E., LaGrave, D., Lamb, A.N., and Toydemir, R.M. (2019). Delineating the Clinical Spectrum Associated With Xq25q26.2 Duplications: Report of 2 Families and Review of the Literature. J. Child Neurol. *34*, 86–93.